Vehicle Classification and Speed Estimation Based on a Single Magnetic Sensor

WENGANG LI, ZHEN LIU, YILONG HUI [ID], LIUYAN YANG, RUI CHEN [ID], AND XIAO XIAO
State Key Laboratory of Integrated Services Networks, Xidian University, Xi'an 710071, China

Corresponding author: Yilong Hui (ylhui@xidian.edu.cn)

ABSTRACT The integration of Internet of things (IoT) and intelligent transportation system (ITS) is expected to improve the traffic efficiency and enhance the driving experience. However, due to the dynamic traffic environment and various types of vehicles, it is a challenge to perform vehicle classification and speed estimation with a single magnetic sensor. In this paper, based on a single low-cost magnetic sensor, a scheme is proposed to achieve vehicle classification and speed interval estimation by designing a two-dimensional convolutional neural network (CNN). Specifically, we extract the magnetic field data of each vehicle and then convert the collected data into a two-dimensional grayscale image. In this way, the images of vehicle signals with different types and driving speeds can be used as the input data to train the designed CNN model. With the designed CNN model, we classify the vehicles into 7 types and estimate the speed interval of each vehicle, where the speeds in the range of 10km/h-70km/h are divided into 6 intervals of size 10km/h. The performance of the proposed vehicle classification and speed estimation scheme is evaluated by experiments, where the experimental results show that the accuracy of vehicle classification and the accuracy of speed interval estimation are 97.83% and 96.85%, respectively.

INDEX TERMS Internet of Things, intelligent transportation system, convolutional neural network, magnetic sensor, vehicle classification, speed estimation.

I. INTRODUCTION

The intelligent transportation system (ITS), which aims to achieve efficient traffic management, is expected to improve traffic efficiency and traveling experience of drivers [1]–[3]. With the deployment of ITS, the traffic accidents, traffic congestion and carbon emissions can be significantly reduced through the sharing of information in the network [4]–[7]. Unlike the conventional transportation system, the key support for building ITS is the data generated by humans, vehicles and the dynamic traffic environment [8]. Based on the collection and analysis of traffic data, the scheduling strategies can be determined to facilitate different vehicular applications such as path planing [9]–[11] and autonomous driving [12]–[15]. As a typical data collection method, vehicle classification and speed estimation can provide the data

to rationalize the construction of traffic roads and reduce the driving risks. One one hand, the data of vehicle classification and speed estimation can be used for setting speed limit and timing traffic signals [16]. On the other hand, with the estimation of vehicle speed, the driving speed can be obtained to guide the behavior of the driver with the target of enhancing the safety.

To obtain the information of vehicle type and speed in the dynamic traffic environment, the Internet of thing (IoT) which can provide various sensors is a promising solution [17]–[19]. The sensors can be simply classified into two types, namely, intrusive sensors (e.g., intrusive loop detectors) and non-intrusive sensors (e.g., radar detectors, ultrasonic detectors, infrared detectors, and video detectors). The installation and maintenance of the intrusive loop detectors require closing lanes, interrupting traffic and causing damage to the road surface. For the non-intrusive sensors, they have relatively high measurement accuracy and usually do

---

The associate editor coordinating the review of this manuscript and approving it for publication was Nan Cheng.
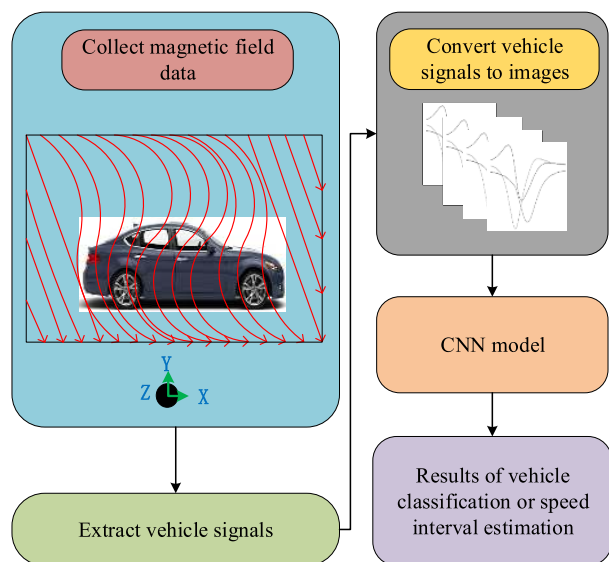
FIGURE 1. Architecture of vehicle classification and speed estimation.

not interfere with the traffic. However, the data collection performance is easily affected by weather conditions. Moreover, these non-intrusive sensors are typically expensive for a large-scale deployment. Compared with these sensors, magnetic sensors have the advantages of sensitive, inexpensive, small size, convenient installation, and immune to weather conditions or environmental factors [20]. As shown in Fig. 1, the basic principle of magnetic sensors is to detect the Earth's magnetic field and extract the magnetic field data. The movement of the vehicle containing a large amount of iron materials (e.g., nickel, iron, and steel) causes disturbance of the Earth's magnetic field, where the magnitude and direction of the disturbance are related to the speed, size, structure and density of the iron materials of the vehicle. By deploying magnetic sensor along the roadside, massive amounts of magnetic field data containing vehicle information can be collected. Therefore, with the processing and analysis of these data, the traffic information such as traffic flow, vehicle types, and vehicle speed can be obtained.

The magnetic sensors have been widely studied for monitoring the dynamic traffic in the ITS, such as vehicle detection on the road [21], vehicle detection in parking lots [22], vehicle classification [23]–[26] and vehicle speed estimation [27]–[30]. However, the current vehicle classification schemes typically use machine learning methods which require pre-processing of vehicle signals, such as noise filtering, feature extraction and feature reduction. On the other hand, the speed estimation schemes are typically based on the calculation of the cross-correlation between two adjacent sensors. This method requires the two sensors to frequently communicate with each other to share the collected data, leading to high energy consumption. In addition, the requirement for clock synchronization of the sensors also poses challenge to design the data collection system.

To this end, in this paper, we develop an effective scheme to achieve vehicle classification and speed estimation through a single magnetic sensor. In the proposed scheme, a convolutional neural network (CNN) model is designed to classify the types of vehicles and estimate the speed range of each vehicle. Specifically, we first design the method to extract the magnetic field data of vehicles based on a single magnetic sensor. Then, we transform the collected vehicle signals into two-dimensional images, where the images are used as the input data of the proposed CNN model. As shown in Fig. 1, the proposed scheme does not require the pre-processing of magnetic signals (e.g., noise filtering, feature extraction and feature reduction). In this way, the proposed CNN model can fully learn the characteristics of vehicle signals with different types or different speeds. As a consequence, the vehicle classification and speed interval estimation can be achieved to facilitate the vehicular applications in the ITS. Our main contributions are three-fold:

- We propose a vehicle classification and speed estimation scheme based on CNN. With this scheme, the signals of each vehicle can be extracted and transformed into a two-dimensional grayscale image.
- Based on the collected images of various vehicles, we design a CNN model to divide the vehicle type and vehicle speed into seven categories and six intervals, respectively.
- We evaluate the proposed scheme with experiments. The results show that the accuracy of vehicle classification and the accuracy of speed interval estimation are 97.83% and 96.85%.

The remainder of this paper is organized as follows. Section II presents the related works. Section III describes the magnetic sensor and introduces the method for extracting vehicle signals. The proposed CNN model for vehicle classification and speed estimation is detailed in section IV. Section V evaluates the performance of the proposed scheme by using experimental results. Section VI closes the paper with conclusions and future work.

II. RELATED WORK
A. VEHICLE CLASSIFICATION
The problem of vehicle classification using magnetic sensors has been studied in a number of works. In [31], a group of magnetic sensors are placed along the roadside for vehicle detection and classification, where vehicles are classified into four groups by estimating their magnetic length. Three magnetic sensors are used in [23] to classify the vehicles that pass in the adjacent lane, where the types of vehicles can be classified by jointly considering the magnetic length and magnetic height of vehicles. With a single-axis magnetic sensor, the authors in [32] develop a classifier based on the improved support vector machine for distinguishing the types of vehicles with three groups. The results show that a 90% classification accuracy can be obtained with the data set of 93 vehicles. In [33], the authors propose a feature selection model for vehicle classification using a single magnetic sensor. With this model, 10 optimal features are selected

to divide vehicles into four-groups. In [25], the authors develop a scheme to achieve vehicle classification according to a 3-axis magnetic sensor in the low-speed congested traffic environment. With this scheme, five signal features are extracted to classify vehicles based on a tree-based algorithm. In [34], the authors propose an algorithm to classify vehicles into six types, where the classification algorithm is of low computational requirements.

B. SPEED ESTIMATION

The speed estimation has been extensively studied in recent years. In [23], based on the calculation of the cross correlation between the signals obtained by two roadside magnetic sensors, the time interval between the vehicle passing by two sensors can be obtained. As a result, the speed of the vehicle can be calculated by dividing the distance between the two sensors by the time interval. In [27], the authors design a region-based algorithm for speed estimation by selecting a region of each signal according to a threshold. In [35], a single roadside node composed of an accelerometer and a magnetic sensor is used to estimate vehicle speed by analyzing magnetic length. The results show that the speed estimation accuracy of the proposed scheme is 90%. In [29], the authors propose a scheme for speed estimation using four magnetic sensor nodes per lane. With this scheme, the error in speed estimation under low speed test is 10%. In [30], a speed estimation scheme is designed based on a single magnetic sensor. This scheme aims to estimate the average speed of a number of passing vehicles. In [28], two magnetic sensors are used for speed estimation and one is used for data fusion, where the results show that the error rate of the speed estimation is 20%.

In the above schemes, there are mainly two methods for vehicle classification based on magnetic sensors. One is classification based on the vehicle magnetic length. This method relies on the estimation of the speed of the vehicle. The other is based on the features of the vehicle magnetic field, where a limited number of features can be extracted to classify the types of vehicles. In addition, the schemes of vehicle speed estimation are mainly implemented by using two or more magnetic sensors. In this way, the speed estimation system suffers from the burdens of the time nchronization and the communication consumption. Different from the above schemes, we propose a scheme to achieve classification and speed estimation with a single magnetic sensor. In the scheme, the signals of each vehicle collected by the sensor are analyzed by using the designed CNN model to achieve vehicle classification and speed estimation.

III. EXTRACT VEHICLE SIGNALS

In this section, we introduce the magnetic sensor used in our paper and then design the vehicle detection algorithm to extract vehicle signals.

The sensor module consists of a central processor and a RM3100 sensor, where the resolution and the rate of the sensor are 26nT and 48MHZ, respectively. Fig. 2 shows the
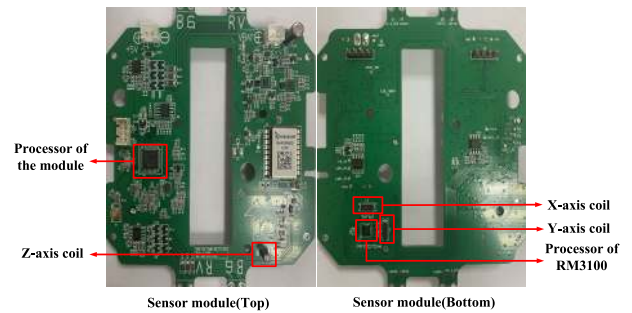

FIGURE 2. Sensor module.

sensor module (i.e., RM3100) which is used to detect the magnetic signals. With this sensor, the magnetic signals of three axes (i.e., *x*, *y* and *z*) can be collected [36]. Before the vehicle classification and speed estimation, the vehicle signals need to be extracted from the data collected by the sensor module. The determination of entering and leaving moments of vehicles have a great impact on the vehicle classification and speed estimation. To this end, we design a state machine for vehicle detection based on a dynamic threshold to determine the state of a vehicle. With the designed state machine, the time when the vehicle enters the detection range and the time when the vehicle exits the detection range of the sensor can be accurately identified. In this way, the vehicle signals can be effectively separated.
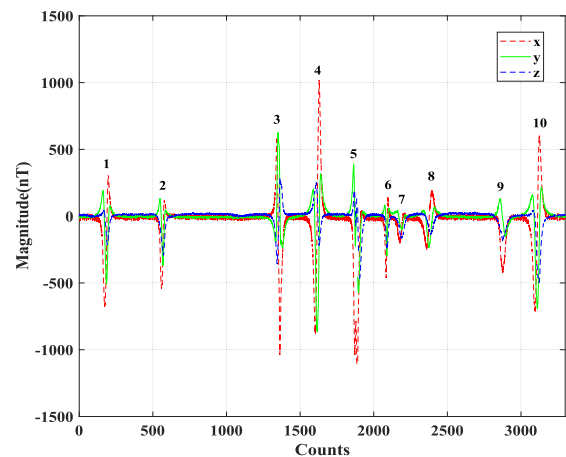

FIGURE 3. Signals of 10 moving vehicles with different axes.

The magnetic signals can be collected from three directions (i.e., *x*, *y* and *z*) by using the magnetic sensor. Fig. 3 shows the variation of the signals of 10 moving vehicles on the three axes. It can be seen from the figure that the magnetic flux lines are pulled away from the reference signal when the vehicle passes the detection coverage of the sensor. In comparison, the magnetic flux lines are pushed back to the reference signal when the vehicle leaves the detection coverage of the sensor. The amplitude and direction of signal fluctuations show different characteristics on different axes. Specifically, vehicles with different types and driving speeds generate different

magnetic signals. In addition, the signal characteristics on different axes of the same vehicle are also different.

We fuse the data collected by the sensor to make full use of the signals of the three axes, shown as

$$
\begin{aligned}
M\,(k) \\
= \sqrt{\left(B_x(k) - b_x(k)\right)^2 + \left(B_y(k) - b_y(k)\right)^2 + \left(B_z(k) - b_z(k)\right)^2},
\end{aligned}
\tag{1}
$$

where k refers to the data collected at the k-th time. $B_x(k)$, $B_y(k)$, and $B_z(k)$ are the signals of the three axes when a vehicle is in the detection coverage of the sensor. $b_x(k)$, $b_y(k)$, and $b_z(k)$ are the reference signals of the three axes, respectively.

After fusing the data, we then extract the vehicle signals with the following steps: 1) Design a dynamic threshold to effectively track the baseline. 2) Design a state machine to determine the arrival and departure moments of the vehicle. 3) Extract vehicle signals.

- **Dynamic threshold to track the baseline**

  The reference magnetic signals are fused as the baseline which changes with the external factors (e.g., temperature and weather). Therefore, it is necessary to track the baseline dynamically to adapt to various traffic environment. To this end, we set a dynamic threshold $Dth(k)$ based on the baseline to decide whether a vehicle is in the detection coverage of the sensor or not. We have

$$
Dth(k) = (1 + \lambda)\,F_{bas}(k), \tag{2}
$$

where $F_{bas}(k)$ is the baseline. λ is the coefficient to adjust the threshold. It can be seen from (2) that the threshold is updated with the baseline in real time. For data $M(k)$, if $M(k) < Dth(k)$, it then can be used to update the baseline. Therefore, the baseline can be tracked by

$$
\begin{aligned}
F_{bas}(k) \\
= \begin{cases} (1-\delta)F_{bas}(k-1) + \delta M(k), & M(k) < Dth(k), \\ F_{bas}(k-1), & M(k) \geq Dth(k), \end{cases}
\end{aligned}
\tag{3}
$$

where δ is the weighting factor to determine the update rate of the baseline.

- **State machine for vehicle detection**

  In order to accurately calculate the time points when the vehicle enters and leaves the detection range of the sensor, as shown in Fig. 4, we design a state machine to model the state of the vehicle. Before using the state machine to make decisions, the value of the collected magnetic signal $M(k)$ needs to be compared with the value of the dynamic threshold $Dth(k)$, we have

$$
ID = \begin{cases} 1, & M(k) \geq Dth(k), \\ 0, & M(k) < Dth(k), \end{cases} \tag{4}
$$

where $ID = 0$ indicates that the vehicle may leave the detection range of the sensor. In comparison, $ID = 1$
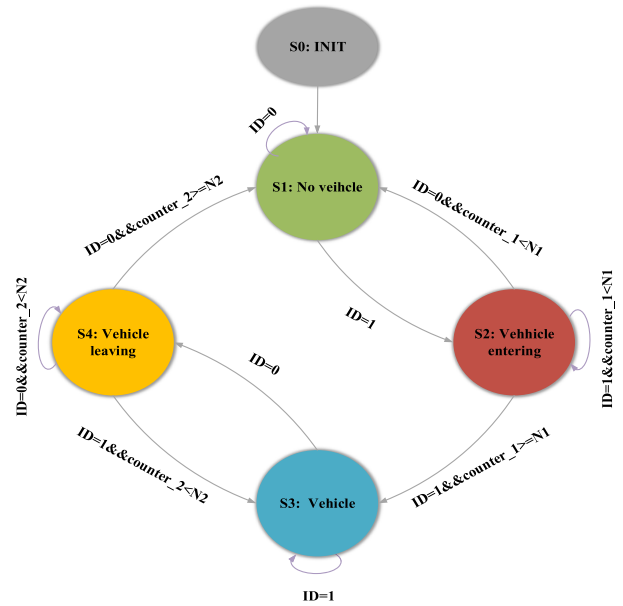

FIGURE 4. State machine for vehicle detection.

means that the vehicle may enter the detection range of the sensor.

In Fig. 4, **S0** state initializes the system and sets the parameters. After the system initialization is completed, the system enters **S1** state and the value of ID is 0. When the collected data is no smaller than the threshold (i.e., $M(k) \geq Dth(k)$), the vehicle may enter the detection coverage of the sensor. At this time, the value of ID is 1 and the state machine moves to **S2**. In this state, counter_1 starts counting and the counting result is compared with the value of $N1$. If counter_1 $\geq N1$, we consider that a vehicle drives in the detection coverage of the sensor. Meanwhile, the state machine moves to **S3**. Otherwise, the value of ID is set to 0 and the state machine returns to **S1**. In state **S3**, when the vehicle signal is lower than the threshold, the vehicle may leave the detection coverage of the sensor. Then, set the value of ID to 0 and the state machine moves to **S4**. In this state, counter_2 starts counting and the counting result is compared with the value of $N2$. If counter_2 $\geq N2$, the vehicle has left from the detection coverage of the sensor and the state machine moves to **S1** state. Otherwise, the value of ID is set to 1 and the state machine moves to **S3**. The vehicle detection result based on the state machine is shown in Fig. 5.

- **Extract vehicle signals**

  Based on the designed state machine for vehicle detection, the time points when the vehicle enters and exits the detection range of the magnetic sensor can be determined. Therefore, as shown in Fig. 6, the signals generated by a vehicle which drives through the detection coverage of the sensor can be effectively segmented from the magnetic signals.
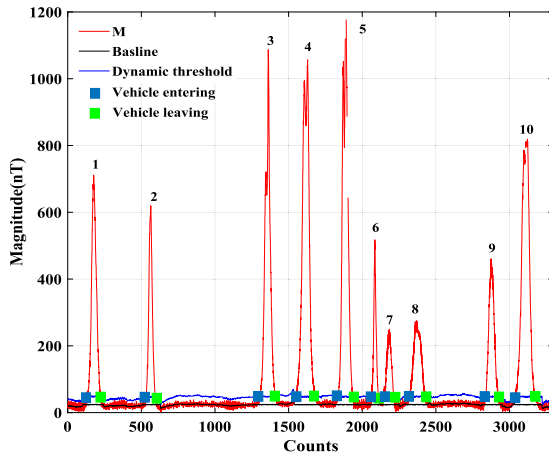
FIGURE 5. The result of vehicle detection.

IV. ANALYSIS AND PROCESSING OF VEHICLE SIGNALS

A. ANALYSIS OF VEHICLE SIGNALS

The magnetic signals of a vehicle is not only related to its structure, but also related to its speed and the cargo loaded, where the structure of the vehicle includes the position of its engine, the height of its chassis and the length of the vehicle. Theoretically, the same vehicles passing by the detection coverage of the sensor at the same speed and direction have almost identical vehicle signals. Unfortunately, in actual traffic scenarios, the speed and position of vehicles passing by the sensor are not exactly the same. For the vehicles with the same type, their vehicle structures are basically the same. However, different vehicle signals are also generated as vehicles usually drive at different speeds. Fig. 7 shows the vehicle signals of three axes collected by the vehicle when passing through the magnetic sensor at 20km/h, 30km/h, 40km/h, and 50km/h, respectively. It can be seen in this figure that the obvious difference is the length of the waveform when the same vehicle moving at different speeds. For vehicles with different types, their structures are different, which results in different vehicle signals. Fig. 8 shows seven different types of vehicle signals, indicating that each type has its unique signal characteristics. Consequently, the vehicle can be classified by collecting and processing the vehicle signals.

B. PROCESSING OF VEHICLE SIGNALS

In this subsection, we convert the data of vehicle signals into two-dimensional images before introducing the CNN model for vehicle classification and speed estimation. The images, which have all the features of the vehicle signals, are treated as the input data to train the CNN model designed in our paper. Based on [31], the types of vehicles are divided into 7 categories which are motorcycles, sedans, SUVs, vans, cranes, medium trucks and buses. After extracting the signals of each vehicle, a two-dimensional figure can be drawn by taking the amplitude of each waveform as the ordinate and the number of points as the abscissa. We draw the three-axis signals of each vehicle on two-dimensional coordinates and
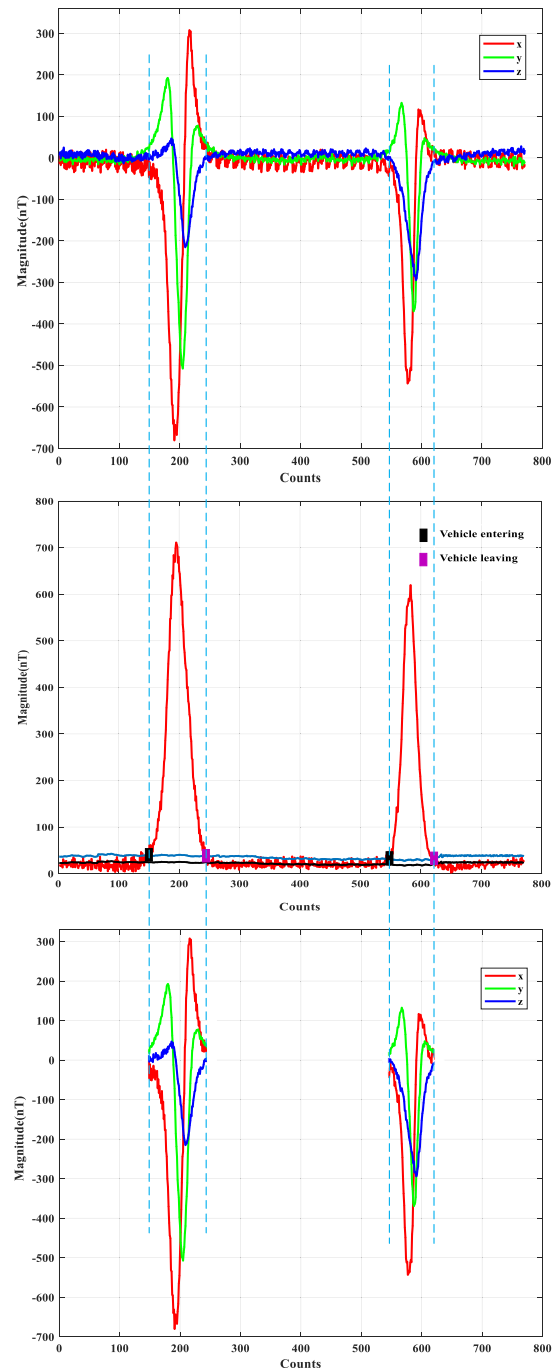

FIGURE 6. The extraction of vehicle signals.

then convert the signals into a 224 × 224 grayscale image. The images transformed by different vehicle signals can be seen in Fig. 9.

V. CNN MODEL FOR VEHICLE CLASSIFICATION AND SPEED ESTIMATION

In our paper, vehicle classification is to make classification labels for vehicle signals according to the type of each vehicle. Similarly, speed interval estimation is to make classification labels for each vehicle according to the speed. Therefore,
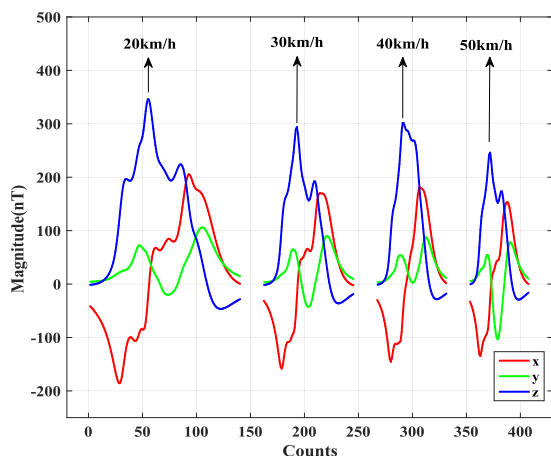
FIGURE 7. Signals collected by the vehicle when passing the magnetic sensor at 20km/h, 30km/h, 40km/h, and 50km/h, respectively.
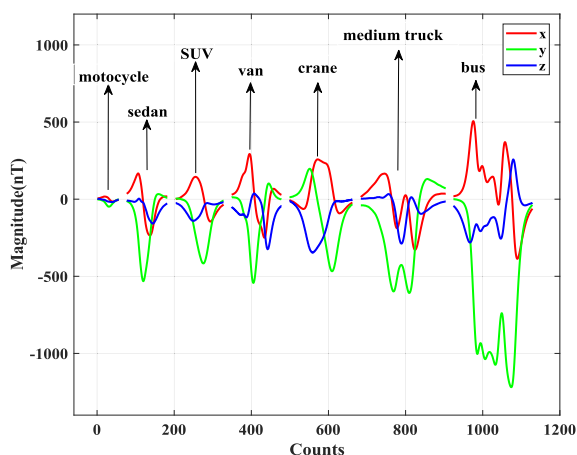

FIGURE 8. Signals generated by the vehicles with different types.
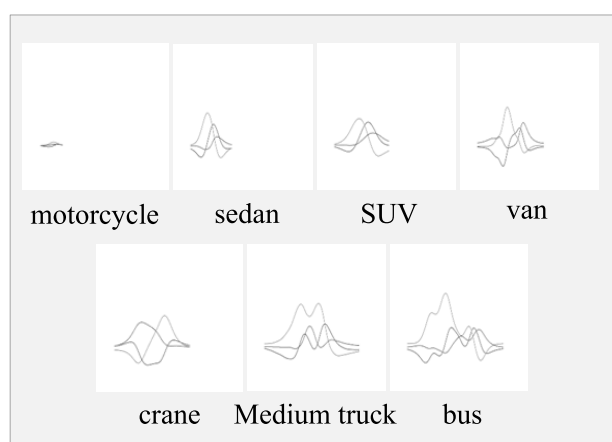

FIGURE 9. Images converted from vehicle signals.

the CNN models for vehicle classification and speed estimation have the same architecture and optimization technology. This section describes the proposed CNN model in detail, including the structure of the model and the optimization techniques, where the optimization techniques respectively

are Xavier initialization, activation function, loss function and optimizer, batch normalization and dropout.
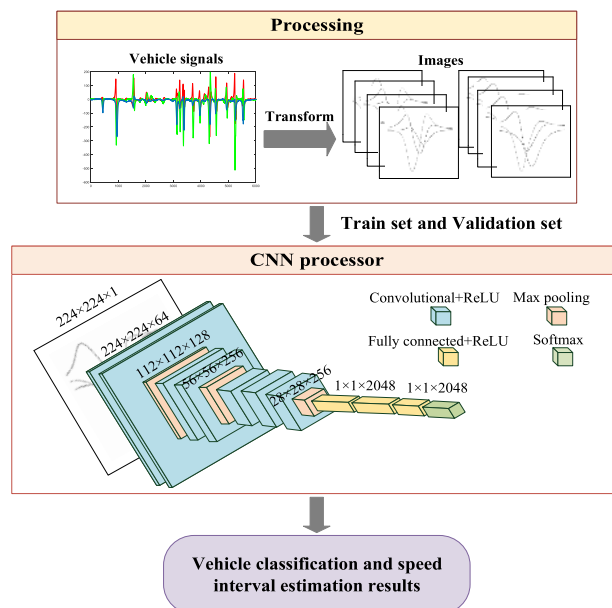

FIGURE 10. Structure of the proposed CNN model for vehicle classification and speed interval estimation.

A. STRUCTURE OF THE PROPOSED CNN MODEL

CNN is a feed-forward neural network, which can directly use the original image as the input, thereby avoiding the complex pre-processing of the image [37]–[39]. In our paper, the CNN model is essentially to learn the characteristics of vehicle signals with the target of achieving vehicle classification and speed estimation. After the vehicle signals are extracted, they will be converted into image data and treated as the input of the CNN models to train the classification model and speed estimation model, respectively. Fig. 10 represents the structure of the proposed CNN model for vehicle classification and speed interval estimation. It can be seen that the CNN model contains 3 groups of convolutions, where each group uses a 3×3 convolution kernel. After each group executes a convolution, a 2×2 maximum pooling is performed. As shown in Fig. 10, the CNN model optimizes various functions to reduce overfitting, thereby showing the best performance of vehicle classification and speed interval estimation. The parameters of the proposed CNN model are summarized in Table 1.

B. XAVIER INITIALIZATION

The purpose of convolution kernel initialization of the CNN model is to let the neural network learn useful information during the training process. However, the initial value cannot be set arbitrarily, otherwise it will cause the problem of gradient instability. For example, the gradient continually decreases with the layer-by-layer transfer of the chain-derivative and finally approaches 0. As a result, some

TABLE 1. Parameters of the proposed CNN model.

Input 224 × 224 grayscale image				
Layer	Kernel size	Stride	Number of kernels	Input size
Conv2D	3 × 3	1	64	224 × 224 × 1
Conv2D	3 × 3	1	64	224 × 224 × 64
Maxpool	2 × 2	2	-	224 × 224 × 64
Conv2D	3 × 3	1	128	112 × 112 × 64
Conv2D	3 × 3	1	128	112 × 112 × 128
Maxpool	2 × 2	2	-	112 × 112 × 128
Conv2D	3 × 3	1	256	56 × 56 × 128
Conv2D	3 × 3	1	256	56 × 56 × 256
Maxpool	2 × 2	2	-	56 × 56 × 256
Full			2048	28 × 28 × 256
Out of vehicle classification			7	2048
Out of speed estimation			6	2048

layers of the CNN model may not be trained. In our paper, we use Xavier initialization to initialize the convolution kernel of the CNN model. With the Xavier initialization, the activation value of each layer and the variance of the state gradient remain the same in the propagation process. Consequently, the problem of the gradient instability can be avoided and the speed of the convergence is accelerated. Define the convolution kernel of the CNN as W, the dimension of the input data of the layer is n and the dimension of the output data of the layer is m. Then all the convolution kernels are initialized in a uniformly manner, shown as

$$W \sim U\left[-\sqrt{\frac{6}{m+n}}, \sqrt{\frac{6}{m+n}}\right]. \tag{5}$$

Compared with a single large-size convolution kernel, multiple small-size convolution kernels can greatly reduce the number of parameters and calculation complexity while maintaining a constant connection. In comparison, when a smaller convolution kernel is used, the characteristics of images may not be able to be expressed. In this paper, the image data of magnetic signals are relatively sparse. Consequently, we select multiple small kernels for convolution, where the size of the initial convolution kernel is set to be 3 × 3. After the operation of the convolution layer, zero padding is adopted to preserve the original size of the image.

C. ACTIVATION FUNCTION
The activation function is used to remain the features and increase the non-linearity of the neural network model. In current CNN models, the commonly used activation functions are logistic sigmoid (Sigmoid), hyperbolic tangent (Tanh), rectified linear units (ReLU), leakage rectified linear units (LReLU), and exponential linear units (ELU). Although Sigmoid is more biologically reasonable than Tanh, the latter is better for training multilayer neural networks. ReLu is able to achieve the best performance with the unsupervised pre-training. However, the derivative of the Relu function in the region of the negative half is 0. This problem can be addressed by LReLU and ELU. In the experiments which are carried out in our paper, ELU has better results than LReLU. Consequently, we select ELU as the activation function,

shown as

$$ELU(x) = \begin{cases} x, & x > 0, \\ \alpha\left(e^x - 1\right), & \text{otherwise,} \end{cases} \tag{6}$$

where α is the adjustment factor.

D. LOSS FUNCTION AND OPTIMIZER
The loss function is used to estimate the degree of the inconsistency between the predicted value and the real value of the model. It is a non-negative real value function. The smaller the value of the loss function, the better the robustness of the model. The loss function can be minimized by adjusting the network parameters of each layer by the optimizer. In our paper, cross-entropy function is used as the loss function for vehicle classification and speed estimation, we have

$$L = -\frac{1}{l} \sum_x [y \ln a + (1 - y) \ln(1 - a)], \tag{7}$$

where l is the number of training data, y is the expected value, and a is the actual value obtained from the output layer.

After deciding the loss function, we then design the learning rate of the CNN model. The current adaptive learning rate optimization algorithms (e.g., AdaGrad, RMSProp, Adam and AdaDelta) aim to design independent adaptive learning rates for different parameters. In our experiments, Adam has a better performance than the others. Therefore, Adam is selected to determine the learning rate. Specifically, in our CNN model, we use the Adam optimizer function with an initial learning rate of 0.0001, which exponentially decays the learning rate with a 0.95 decay rate every 1000 steps. The learning rate can be calculated by

$$\text{LearnR} = \text{LearnR}_0 * 0.95^{\lceil (\text{GlobalStep}/1000) \rceil}, \tag{8}$$

where $\lceil \cdot \rceil$ is the ceil function.

E. BATCH NORMALIZATION
CNN involves the superposition of many layers, where the update of the parameters of each layer will change the distribution of the input data at the upper layer. The distribution of the input data at the high layers will change drastically with layer-by-layer superposition, which makes the high layers need to constantly re-adapt the update of the parameters at the low layers. As a common and effective method to address this problem, batch normalization is used to forcibly pull the distribution of the input value of any neuron in each layer back to a standard normal distribution with a mean of 0 and a variance of 1, which can greatly speed up the training speed. In our paper, the batch normalization layer is placed after the activation function.

F. DROPOUT
The CNN model used in our paper has a large number of parameters. In order to reduce the over-fitting of the model, the dropout technology is used in the model training process. With this technology, for the neural network unit, it will

temporarily withdraw from the network according to a certain probability. For the remaining neurons, they will form a new network structure. Finally, the estimates or predictions from different network structures are averaged through a certain weight to obtain the final result. This technology not only solves the over-fitting problem brought by the training of a single model, but also reduces the time consumption when training multiple models. In this paper, we apply a deletion with a probability of 0.5 and place it behind the batch normalization layer.
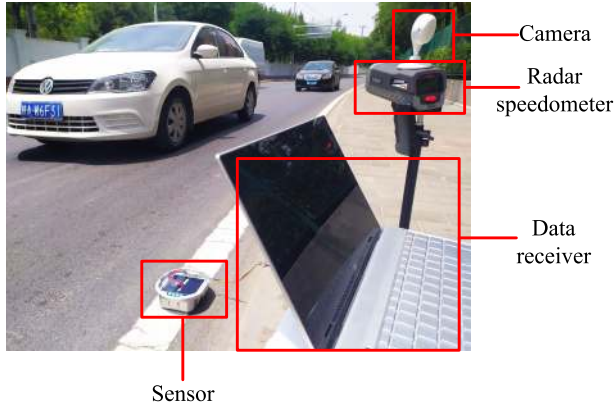

FIGURE 11. The experimental scenario.

VI. EXPERIMENTS AND RESULTS

A. EXPERIMENTAL SCENARIO

In this subsection, we introduce the scenario for carrying out the simulation experiments. In the experiments, we collect the data from three different roads in Xi'an, China to train the CNN model. As shown in Fig. 11, the magnetic sensor is deployed along the road to collect data, where the x-axis is along the traffic direction, y-axis is perpendicular to the traffic direction and z-axis is perpendicular to the ground. In addition, a camera is used to record the type of each vehicle and a radar speedometer is used to record the speed of the vehicle passing by the detection coverage of the magnetic sensor. After the data of the three axes are collected by the magnetic sensor, the data will be delivered from the sensor to the data collection node, i.e., the computer in Fig. 11. Then, the time points of the vehicle arrival and vehicle departure from the sensor detection range can be obtained by the vehicle detection algorithm. After that, the signals of each vehicle can be transmitted into an image to train the CNN model. The original data set has a total of 6042 images, including 396 motorcycles, 1504 sedan, 1435 SUVs, 1201 vans, 331 cranes, 311 medium trucks and 864 buses. The data is expanded by the data enhancement method, and finally we obtain 54378 images of vehicles [40].

B. EXPERIMENTAL RESULTS

1) RESULTS OF VEHICLE CLASSIFICATION

To evaluate the performance of the proposed vehicle classification scheme, we select the commonly used performance metrics which are accuracy, precision, sensitivity, specificity,

and area under the ROC curve (AUC). In the experiments, we use different labels to indicate motorcycles, cars, SUVs, trucks, cranes, medium trucks, and buses. For a type of vehicles, we define the following concepts to calculate the performance metrics.

- **True Positive** *TP*: the number of samples which belong to this type and are correctly classified.
- **False Negative** *FN*: the number of samples which do not belong to this type and are incorrectly classified as this type.
- **False Positive** *FP*: the number of samples which belong to this type and are incorrectly classified into other types.
- **True Negative** *TN*: the number of samples which do not belong to this type and are correctly classified into other types.

In this way, the accuracy, precision, sensitivity and specificity can be calculated by

$$\begin{cases} \text{Accuracy} = \dfrac{TP + TN}{TP + TN + FP + FN}, \\ \text{Precision} = \dfrac{TP}{TP + FP}, \\ \text{Sensitivity} = \dfrac{TP}{TP + FN}, \\ \text{Specificity} = \dfrac{TN}{TN + FP}. \end{cases} \quad (9)$$

Based on (9), we then define the AUC. For a specific classifier and a test data set, a series sets of $\left(\frac{FP}{TN+FP}, \frac{TP}{TP+FN}\right)$ can be obtained by setting different classification thresholds. By plotting these values of $\left(\frac{FP}{TN+FP}, \frac{TP}{TP+FN}\right)$ in a two-dimensional coordinate system, the ROC curve can be obtained, where the AUC is the area under the ROC curve.

TABLE 2. Results of vehicle classification.

	moto	sedan	SUV	van	crane	medium trucks	bus
Accuracy	100%	94.43%	95.68%	97.81%	98.59%	98.86%	99.44%
AUC	0.999	0.938	0.946	0.973	0.981	0.987	0.990
Precision	0.999	0.912	0.923	0.987	0.988	0.994	0.993
Sensitivity	1.000	0.944	0.957	0.978	0.986	0.989	0.994
Specificity	0.994	0.996	0.989	0.994	0.991	0.995	0.997

With these performance metrics, we then detail the experimental results of vehicle classification, where the results of vehicle classification are summarized in Table 2. It can be seen from this Table that the classification performance of motorcycles is the best with an accuracy rate of 100%. In addition, the classification accuracy of buses is 99.44%. The worst performances are sedans and SUVs, their accuracy rates are both lower than 96%. This is because motorcycle has small size and the disturbance generated by motorcycle is weak. As a result, the amplitude of the vehicle signal is low and the duration is short. Compared with other types of vehicles, buses have a stronger disturbance to the magnetic field, a higher signal amplitude and a longer signal duration. Consequently, the vehicle signals of motorcycles and buses are quite different from the signals of other vehicle types.

However, the signals of some sedans and SUVs are similar, which causes the model to be comparatively fuzzy in the recognition of these two types. Fig. 12 shows the accuracy rate and the loss rate of vehicle classification. It can be seen in this figure that the accuracy rate of the training set is 98.57% and the accuracy rate of the validation set is 97.83% after running 80 steps. In addition, the loss of the training set is 0.0612 and that of the validation set is 0.0737 after 80 steps.
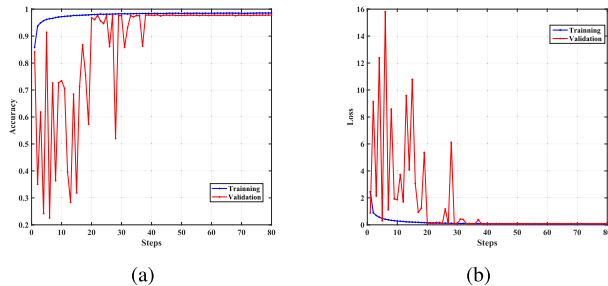

FIGURE 12. Accuracy rate and loss rate of vehicle classification. (a) The accuracy rate of training set and validation set. (b) The loss of training set and validation set.
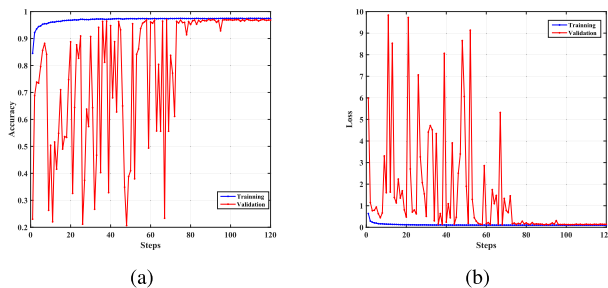

FIGURE 13. Accuracy rate and loss rate of speed interval estimation. (a) The accuracy rate of training set and validation set. (b) The loss of training set and validation set.

2) RESULTS OF SPEED INTERVAL ESTIMATION

To evaluate the speed of a vehicle, the speed in the range of 10km/h-70km/h is divided into 6 intervals with a size of 10 km/h, i.e., [10km/h,20km/h], (20km/h-30km/h], (30km/h-40km/h], (40km/h-50km/h], (50km/h-60km/h] and (60km/h-70km/h]. Then, the collected data of each vehicle is labeled with a classification label according to the speed of the vehicle. After that, the signals of vehicles are converted into images and treated as the input of the CNN model for speed interval estimation. Fig. 13 shows the result of speed interval estimation with the adoption of the proposed scheme. It can be seen in this figure that the accuracy of the speed interval estimation is 96.85%. Furthermore, we can see that the loss of the training set is 0.098 and that of the validation set is 0.136 after 120 steps.

VII. CONCLUSION

The vehicle classification and speed estimation are the basic applications to support the ITS. In this paper, we have proposed an effective scheme for vehicle classification and speed interval estimation based on a single low-cost magnetic sensor. In the proposed scheme, vehicle signals are first extracted from the magnetic signals by using the designed state machine. Then, the collected vehicle signals are converted into 224×224 grayscale images. These images are used as the input to the proposed CNN model. With the designed CNN model, we have classified the vehicles into 7 types and divided the speed in the range of 10km/h-70km/h into 6 intervals with a size of 10km/h. The experimental results have shown that the accuracy of vehicle classification is 97.83% and the accuracy of speed interval estimation is 96.85%.

For the future work, a vehicle detection system including sensor, base station and data analysis platform will be designed to further enhance the performance of the proposed vehicle classification and speed estimation scheme.

REFERENCES

[1] Y. Zhang, G. Zhang, R. Fierro, and Y. Yang, "Force-driven traffic simulation for a future connected autonomous vehicle-enabled smart transportation system," *IEEE Trans. Intell. Transp. Syst.*, vol. 19, no. 7, pp. 2221–2233, Jul. 2018.

[2] C. Chen, L. Liu, T. Qiu, D. O. Wu, and Z. Ren, "Delay-aware grid-based geographic routing in urban VANETs: A backbone approach," *IEEE/ACM Trans. Netw.*, vol. 27, no. 6, pp. 2324–2337, Dec. 2019.

[3] M. Veres and M. Moussa, "Deep learning for intelligent transportation systems: A survey of emerging trends," *IEEE Trans. Intell. Transp. Syst.*, early access, Jul. 24, 2019, doi: 10.1109/TITS.2019.2929020.

[4] Y. Hui, Z. Su, and T. H. Luan, "Collaborative content delivery in software-defined heterogeneous vehicular networks," *IEEE/ACM Trans. Netw.*, vol. 28, no. 2, pp. 575–587, Apr. 2020.

[5] N. Cheng, W. Quan, W. Shi, H. Wu, Q. Ye, H. Zhou, W. Zhuang, X. S. Shen, and B. Bai, "A comprehensive simulation platform for space-air-ground integrated network," *IEEE Wireless Commun.*, vol. 27, no. 1, pp. 178–185, Feb. 2020.

[6] C. Chen, L. Liu, T. Qiu, Z. Ren, J. Hu, and F. Ti, "Driver's intention identification and risk evaluation at intersections in the Internet of vehicles," *IEEE Internet Things J.*, vol. 5, no. 3, pp. 1575–1587, Jun. 2018.

[7] Y. Hui, Z. Su, T. H. Luan, and J. Cai, "A game theoretic scheme for optimal access control in heterogeneous vehicular networks," *IEEE Trans. Intell. Transp. Syst.*, vol. 20, no. 12, pp. 4590–4603, Dec. 2019.

[8] L. Zhu, F. R. Yu, Y. Wang, B. Ning, and T. Tang, "Big data analytics in intelligent transportation systems: A survey," *IEEE Trans. Intell. Transp. Syst.*, vol. 20, no. 1, pp. 383–398, Jan. 2019.

[9] W. Gong, B. Zhang, and C. Li, "Location-based online task assignment and path planning for mobile crowdsensing," *IEEE Trans. Veh. Technol.*, vol. 68, no. 2, pp. 1772–1783, Feb. 2019.

[10] B. Irani, J. Wang, and W. Chen, "A localizability constraint-based path planning method for autonomous vehicles," *IEEE Trans. Intell. Transp. Syst.*, vol. 20, no. 7, pp. 2593–2604, Jul. 2019.

[11] C. Guo, D. Li, G. Zhang, and M. Zhai, "Real-time path planning in urban area via VANET-assisted traffic information sharing," *IEEE Trans. Veh. Technol.*, vol. 67, no. 7, pp. 5635–5649, Jul. 2018.

[12] H. Peng, Q. Ye, and X. S. Shen, "SDN-based resource management for autonomous vehicular networks: A multi-access edge computing approach," *IEEE Wireless Commun.*, vol. 26, no. 4, pp. 156–162, Aug. 2019.

[13] Q. Luo, Y. Cao, J. Liu, and A. Benslimane, "Localization and navigation in autonomous driving: Threats and countermeasures," *IEEE Wireless Commun.*, vol. 26, no. 4, pp. 38–45, Aug. 2019.

[14] Z. Su, Y. Hui, and T. H. Luan, "Distributed task allocation to enable collaborative autonomous driving with network softwarization," *IEEE J. Sel. Areas Commun.*, vol. 36, no. 10, pp. 2175–2189, Oct. 2018.

[15] H. Peng, D. Li, K. Abboud, H. Zhou, H. Zhao, W. Zhuang, and X. Shen, "Performance analysis of IEEE 802.11p DCF for multiplatooning communications with autonomous vehicles," *IEEE Trans. Veh. Technol.*, vol. 66, no. 3, pp. 2485–2498, Mar. 2017.

[16] Y.-K. Ki and D.-K. Baik, "Model for accurate speed measurement using double-loop detectors," *IEEE Trans. Veh. Technol.*, vol. 55, no. 4, pp. 1094–1101, Jul. 2006.

[17] Z. Sheng, H. Wang, C. Yin, X. Hu, S. Yang, and V. C. M. Leung, "Lightweight management of resource-constrained sensor devices in Internet of Things," *IEEE Internet Things J.*, vol. 2, no. 5, pp. 402–411, Oct. 2015.

[18] Z. Sun, G. Bebis, and R. Miller, "On-road vehicle detection: A review," *IEEE Trans. Pattern Anal. Mach. Intell.*, vol. 28, no. 5, pp. 694–711, May 2006.

[19] Y. Hui, Z. Su, and S. Guo, "Utility based data computing scheme to provide sensing service in Internet of Things," *IEEE Trans. Emerg. Topics Comput. Intell.*, vol. 7, no. 2, pp. 337–348, Apr. 2019.

[20] A. Haoui, R. Kavaler, and P. Varaiya, "Wireless magnetic sensors for traffic surveillance," *Transp. Res. C, Emerg. Technol.*, vol. 16, no. 3, pp. 294–306, Jun. 2008.

[21] W. Balid, H. Tafish, and H. H. Refai, "Development of portable wireless sensor network system for real-time traffic surveillance," in *Proc. IEEE ITSC*, Sep. 2015, pp. 1630–1637.

[22] H. Zhu and F. Yu, "A vehicle parking detection method based on correlation of magnetic signals," *Int. J. Distrib. Sensor Netw.*, vol. 11, no. 7, Jul. 2015, Art. no. 361242.

[23] S. Taghvaeeyan and R. Rajamani, "Portable roadside sensors for vehicle counting, classification, and speed measurement," *IEEE Trans. Intell. Transp. Syst.*, vol. 15, no. 1, pp. 73–83, Feb. 2014.

[24] H. Li, H. Dong, L. Jia, and M. Ren, "Vehicle classification with single multi-functional magnetic sensor and optimal MNS-based CART," *Measurement*, vol. 55, pp. 142–152, Sep. 2014.

[25] B. Yang and Y. Lei, "Vehicle detection and classification for low-speed congested traffic with anisotropic magnetoresistive sensor," *IEEE Sensors J.*, vol. 15, no. 2, pp. 1132–1138, Feb. 2015.

[26] W. Ma, D. Xing, A. McKee, R. Bajwa, C. Flores, B. Fuller, and P. Varaiya, "A wireless accelerometer-based automatic vehicle classification prototype system," *IEEE Trans. Intell. Transp. Syst.*, vol. 15, no. 1, pp. 104–111, Feb. 2014.

[27] D.-H. Kim, K.-H. Choi, K.-J. Li, and Y.-S. Lee, "Performance of vehicle speed estimation using wireless sensor networks: A region-based approach," *J. Supercomput.*, vol. 71, no. 6, pp. 2101–2120, Jun. 2015.

[28] D. Nan, T. Guozhen, M. Honglian, L. Mingwen, and S. Yao, "Low-power vehicle speed estimation algorithm based on WSN," in *Proc. IEEE ITSC*, Oct. 2008, pp. 1015–1020.

[29] L. Zhang, R. Wang, and L. Cui, "Real-time traffic monitoring with magnetic sensor networks," *J. Inf. Sci. Eng.*, vol. 27, no. 4, pp. 1473–1486, 2011.

[30] X. Deng, Z. Hu, P. Zhang, and J. Guo, "Vehicle class composition identification based mean speed estimation algorithm using single magnetic sensor," *J. Transp. Syst. Eng. Inf. Technol.*, vol. 10, no. 5, pp. 35–39, Oct. 2010.

[31] W. Balid, H. Tafish, and H. H. Refai, "Intelligent vehicle counting and classification sensor for real-time traffic surveillance," *IEEE Trans. Intell. Transp. Syst.*, vol. 19, no. 6, pp. 1784–1794, Jun. 2018.

[32] J. Lan, Y. Xiang, L. Wang, and Y. Shi, "Vehicle detection and classification by measuring and processing magnetic signal," *Measurement*, vol. 44, no. 1, pp. 174–180, Jan. 2011.

[33] Y. He, Y. Du, L. Sun, and Y. Wang, "Improved waveform-feature-based vehicle classification using a single-point magnetic sensor," *J. Adv. Transp.*, vol. 49, no. 5, pp. 663–682, Aug. 2015.

[34] S. Y. Cheung, S. Coleri, B. Dundar, S. Ganesh, C.-W. Tan, and P. Varaiya, "Traffic measurement and vehicle classification with single magnetic sensor," *Transp. Res. Rec., J. Transp. Res. Board*, vol. 1917, no. 1, pp. 173–181, Jan. 2005.

[35] D. Obertov, V. Bardov, and B. Andrievsky, "Vehicle speed estimation using roadside sensors," in *Proc. ICUM*, Oct. 2014, pp. 111–117.

[36] Z. Chen, Z. Liu, Y. Hui, W. Li, C. Li, T. H. Luan, and G. Mao, "Roadside sensor based vehicle counting in complex traffic environment," in *Proc. IEEE Globecom Workshops*, Dec. 2019, pp. 1–5.

[37] Y. Liu, C. Y. Suen, Y. Liu, and L. Ding, "Scene classification using hierarchical Wasserstein CNN," *IEEE Trans. Geosci. Remote Sens.*, vol. 57, no. 5, pp. 2494–2509, May 2019.

[38] R. Dong, D. Xu, J. Zhao, L. Jiao, and J. An, "Sig-NMS-based faster R-CNN combining transfer learning for small target detection in VHR optical remote sensing imagery," *IEEE Trans. Geosci. Remote Sens.*, vol. 57, no. 11, pp. 8534–8545, Nov. 2019.

[39] C. Yang, B. Hou, B. Ren, Y. Hu, and L. Jiao, "CNN-based polarimetric decomposition feature selection for PolSAR image classification," *IEEE Trans. Geosci. Remote Sens.*, vol. 57, no. 11, pp. 8796–8812, Nov. 2019.

[40] L. Perez and J. Wang, "The effectiveness of data augmentation in image classification using deep learning," 2017, *arXiv:1712.04621*. [Online]. Available: http://arxiv.org/abs/1712.04621

WENGANG LI received the B.Sc. and Ph.D. degrees in communication and information systems from Xidian University, Xi'an, China, in 2004 and 2010, respectively. He is currently an Associate Professor with the School of Communication Engineering, Xidian University. His research interests include navigation and positioning, broadband wireless communication, massive MIMO technology, networking technology, and its application.

ZHEN LIU received the bachelor's degree from Xidian University, Xi'an, China, where she is currently pursuing the master's degree with the School of Telecommunication Engineering. Her research interests are the Internet of Vehicles, machine learning, deep neural networks, data mining, and intelligent transportation systems.

YILONG HUI received the Ph.D. degree in control theory and control engineering from Shanghai University, Shanghai, China, in 2018. He is currently a Lecturer with the State Key Laboratory of Integrated Services Networks and with the School of Telecommunication Engineering, Xidian University, China. He has published more than 20 scientific articles in leading journals and international conferences, including the IEEE JOURNAL ON SELECTED AREAS IN COMMUNICATIONS, the IEEE/ACM TRANSACTIONS ON NETWORKING, the IEEE TRANSACTIONS ON INTELLIGENT TRANSPORTATION SYSTEMS, the IEEE TRANSACTIONS ON VEHICULAR TECHNOLOGY, the IEEE TRANSACTIONS ON EMERGING TOPICS IN COMPUTING, and the IEEE WIRELESS COMMUNICATIONS. His research interests include wireless network architecture, mobile edge computing, vehicular networks, autonomous driving, and intelligent transportation systems.

LIUYAN YANG received the bachelor's degree from Xidian University, where he is currently pursuing the master's degree with the School of Telecommunication Engineering. His research interests are communication technology and massive MIMO technology.

RUI CHEN received the B.S., M.S., and Ph.D. degrees in communications and information systems from Xidian University, Xi'an, China, in 2005, 2007, and 2011, respectively. From 2014 to 2015, he was a Visiting Scholar with Columbia University, New York City, NY, USA. He is currently an Associate Professor and a Ph.D. Supervisor of the School of Telecommunications Engineering, Xidian University. He has published about 50 papers in international journals and conferences and held ten patents. His research interests include broadband wireless communication systems, array signal processing, and intelligent transportation systems. He is also an Associate Editor of the *International Journal of Electronics, Communications, and Measurement Engineering* (IGI Global) and a reviewer of a number of international journals and conferences, including the IEEE, Springer, and Elsevier.

XIAO XIAO received the B.S. degree in control technology and instrumentation from Xidian University, Xi'an, China, in 2004, and the Ph.D. degree in measuring and testing technologies and instruments from Zhejiang University, Hangzhou, China, in 2009. He was a Research Fellow with the Min H. Kao Department of Electrical Engineering and Computer Science, University of Tennessee, in 2019. He is currently a Lecturer with the School of Telecommunication Engineering, Xidian University. His research interests include wireless network architecture, intelligent transportation systems, computer vision, and deep learning.

· · ·